THREE-AXIS REACTION WHEEL ATTITUDE CONTROL SYSTEM FOR KITSAT-3 MICROSATELLITE

B.J. KIM, H. LEE and S.D. CHOI

Satellite Technology Research Center, KAIST, Taejon, 305-701, Korea

Abstract : A design study of the low cost attitude control system for the KITSAT-3 microsatellite has been done to achieve high precision control performance. Three-axis reaction wheel and fiber optic rate gyro system with magnetorquers was proposed for the control hardwares of the satellite. The system is specially designed for a low earth orbit budget mission. Star sensor and rate gyro combination will provide high accuracy attitude reference while the satellite is in the precision pointing mode. Modeling of the spacecraft dynamics and comparison between conventional quaternion feedback and genetic algorithm are presented with simulation results.

Keywords: Attitude control; wheel; gyro; genetic algorithm.

1. INTRODUCTION

After the successful launches and operations of two microsatellites, the KITSAT-1 and 2, the Satellite Technology Research Center (SaTReC) is developing the next generation microsatellite the KITSAT-3. Two predecessors are gravity-gradient stabilized spacecrafts with 3-axis on-off type magnetorquers, which have 5 degree attitude pointing accuracy. The attitude control system of the KITSAT-3 was proposed to accommodate high attitude accuracy and stability requiring payloads.

The KITSAT-3 is designed to meet 45×45×78cm of volume and 100kg of weight constraints. Two deployable solar arrays are employed to generate appropriate power for the operation. The main objectives of the mission are to develop 3-axis stabilized satellite bus system, high speed communication system, push broom type remote sensing camera, particle detector and electron temperature probe. Figure 1. shows the out view and operation of KITSAT-3.

During the normal operation mode the satellite is facing the sun for maximum power generation and it rotates about the pitch axis for Earth imaging. For the scientific payload, the particle telescope, a constant pitch rate of 0.5 r.p.m. is required.

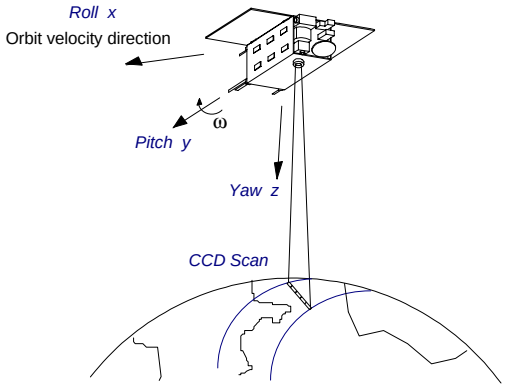

Fig. 1. KITSAT-3 out view and operation

The CCD camera with 15m ground pixel resolution demands the most stringent attitude control requirements in the mission. At the proposed 800km 10:30 sun synchronous orbit 0.5 degree pointing accuracy with 0.014 deg/sec stability of the platform has to be achieved for quality images. Basically all the proposed operation modes are controllable with the pitch torque. However, due to 22.5° tilt along the roll axis for maximum solar power, 3-axis reaction wheel system's controllability outweighs the simplicity of a single momentum wheel system.

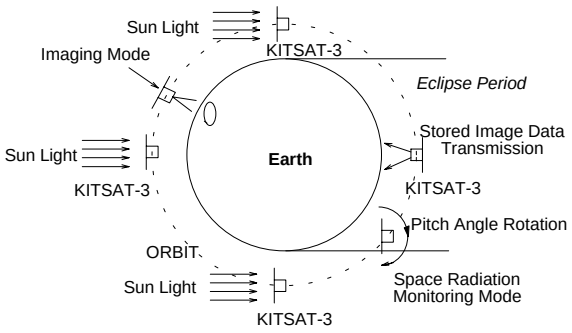

Fig. 2. Operation modes of KITSAT-3

The spacecraft will be in normal sun pointing mode most of the times. Attitude maneuvers are required prior to the imaging mode. During the camera operation the *y* rate ω is maintained as the orbit rate, 100 minutes, with the *z* axis pointing to nadir. 22.5° rotation along the *x* axis has to be done with the pitch control.

2. KITSAT-3 ATTITUDE CONTROL SYSTEM STRUCTURE

The attitude motion of the satellite is monitored by five different types of sensors, magnetometer, sun sensor, Earth horizon sensor, fiber optic gyro and star sensor. The fiber optic gyros are regularly updated from the accurate information provided by the star sensor to compensate drifts. For small power budget Teldix's gyro (MFK 4-0 type) that consumes 3W power has been selected.

Unlike the on-off type magnetorquers on the KITSAT-1 and 2, which can be operated one axis at a time, a simultaneous driving scheme of 3-axis air type magnetic coils with 256 level quantization is a new feature in the KITSAT-3. The reaction wheel (DR01 type) manufactured by Teldix is an attractive choice for microsatellites since it consumes only 1W and weighs 1kg. However, due to the small momentum storage capacity of the wheel, 0.1N·m·sec, the magnetorquers occasionally need to dump wheel momentum to prevent saturation.

The attitude control processor (KASCOM) is an Intel 80960MC CPU based computer which can handle 2 MIPS. Its reliability has been proven after three years of operation in space on the KITSAT-2. Each subsystem is connected to the Modular Telemetry and Command (MTC) network to share communication, tele-commands and telemetry information. The shared bus structure is a modification of MIL-STD-1553B bus. Fig. 3 shows the KITSAT-3 attitude control system structure.

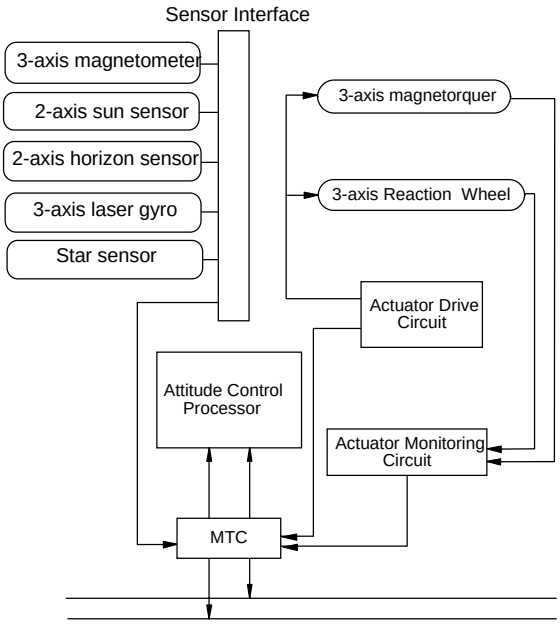

Fig. 3. Attitude control system block diagram

3. DISTURBANCE ANALYSIS

The KITSAT-3 has been modeled as 22 separate modules to acquire its mechanical properties. The result shows that the center of mass is located at 238mm from the bottom plate in the direction of -*y* axis with 201mm and 217mm displacements from its geometrical center for the -*x* and -*z* axis, respectively. The moments of inertia for the principle axes are evaluated as I_x=3.118, I_y=3.05, and I_z=4.055 kg·m^2 .

During the sun tracking mode the satellite is rotated 22.5° with respect to the *x* axis. Therefore, a secular term exists along the *x* axis in the gravity gradient torque model. Solar pressure gives non-periodic torques to *x* and *y* axes. Aerodynamic torque is periodic along all the three axes. Summing up all these disturbance sources gives environmental torque model eq. (1) (Hughes, 1986).

$$\begin{aligned} T_x &= a\cos^2\omega_o t + b + c\cos(\omega_o t - \pi/2) \\ T_y &= d\sin 2\omega_o t + e + \cos\omega_o t + f\cos(\omega_o t - \pi/2) \\ T_z &= g\sin 2\omega_o t + h\cos\omega_o t \end{aligned} \quad (1)$$

,where the time *t* is measured from the ascending node, ω_o is the orbit rate 0.001 rad/sec and constant coefficients are given according to the spacecraft configuration and attitude. Averaging over an orbit period, 100 minutes, results in secular components in the disturbance torque terms. *x* component is 3.19×10^{-7}, and that of *y* is 6.08×10^{-9} N·m. T_z averages to 0 as expected. After an orbit period the *x* and *y* reaction wheel gain speed of 76 and 1.47 r.p.m if eclipse condition is excluded. Fig. 4. is a simulation result of the environmental torques over 1 orbit period.

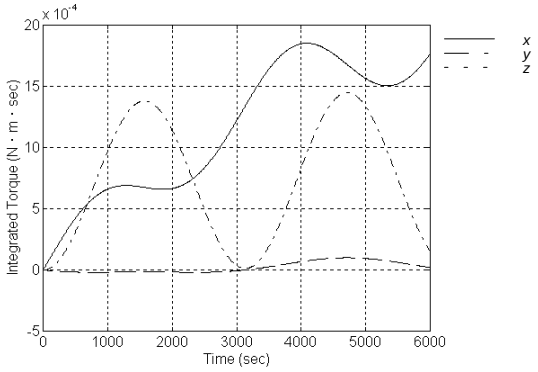

Fig. 4. Integrated environmental torques during the sun tracking mode

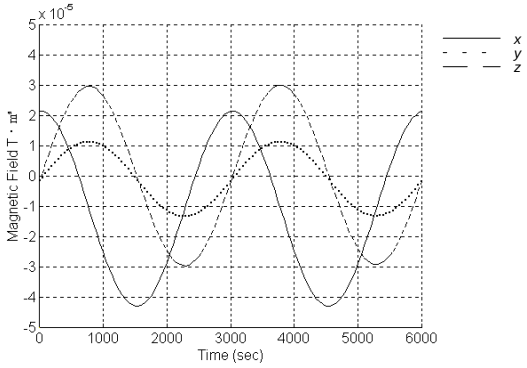

Fig. 5. Geomagnetic field in the sun tracking mode

4. ATTITUDE DYNAMICS

When the reaction wheels are stationary the attitude motion of a rigid body satellite can be described by the well known Euler's equation in the spacecraft body referenced frame in eq. (2) (Kaplan, 1976).

$$\begin{aligned} I_x\omega_x' + \omega_y\omega_z(I_z - I_y) &= T_x \\ I_y\omega_y' + \omega_x\omega_z(I_x - I_z) &= T_y \\ I_z\omega_z' + \omega_x\omega_y(I_y - I_x) &= T_z \end{aligned} \tag{2}$$

Identical three reaction wheels located along the principle axes affect the attitude motion. A wheel has a moment of inertia of I_w=2.39×10^{-4} kg·m^2. Let the angular speed of the wheels are Ω_x, Ω_y and Ω_x along the x, y, and z axes, respectively. The effect of the angular momentum vector derivative of the reaction wheel system $\vec{h}_w' = I_w(\Omega_x\vec{i} + \Omega_y\vec{j} + \Omega_z\vec{k})'$ has to be considered for the complete motion equation eq. (3).

$$\begin{aligned} I_x\omega_x' + \omega_y\omega_z(I_z - I_y) + I_w(\Omega_z\omega_y - \Omega_y\omega_z + \Omega_x') &= T_x \\ I_y\omega_y' + \omega_x\omega_z(I_x - I_z) + I_w(\Omega_x\omega_z - \Omega_z\omega_x + \Omega_y') &= T_y \\ I_z\omega_z' + \omega_x\omega_y(I_y - I_x) + I_w(\Omega_y\omega_x - \Omega_x\omega_y + \Omega_z') &= T_z \end{aligned} \tag{3}$$

5. MOMENTUM DUMPING

As the spacecraft moves in the orbit during the sun tracking mode the momentum of the reaction wheel, especially the x axis one, builds up due to the environmental torques. Occasional momentum dumping is necessary by means of the magnetorquers.

However, the controllability of the magnetorquers are severely limited by the given geomagnetic field condition. Unlike the Earth pointing case the geomagnetic field components in the satellite body fixed frame in the sun tracking mode vary with the half of the orbit period as depicted in Fig. 5.

KITSAT-3 has magnetic dipole capacity of 10.4 Am^2 for y and 12 Am^2 for x and z axes. A simple algorithm to generate magnetic momentum for the momentum unloading is to operate magnetorquers when the geomagnetic field is near zero along the axis the momentum to be dumped. It eliminates momentum change possibilities in the unwanted directions. Such opportunities are available four times an orbit period as shown in Fig. 5.

For the maximum torque condition the magnetic dipole vectors have to be controlled carefully. The x axis is likely to be the controlled most of the time since the x disturbance torque is the dominant one. When the geomagnetic field B_x is near zero the magnetic dipole component m_x of the magnetic torquer has to be close to zero too. Therefore, the resultant torques in the y and z direction are relatively small compared to that of x. One remaining problem is to maximize the torque T_x and minimize T_y and T_z.

Even though the given geomagnetic field has non-negligible x component, momentum unloading can be still performed. A simple rule is to give weighting values to the desired magnetic torques according to the errors between the target and the observed wheel speeds $\Delta\Omega$.

$$\begin{aligned} T_x &= (m_yB_z - m_zB_y)\Delta\Omega_x \\ T_y &= (m_zB_x - m_xB_z)\Delta\Omega_y \\ T_z &= (m_xB_y - m_yB_x)\Delta\Omega_z \end{aligned} \tag{4}$$

The unit vector components m_{xo}, m_{yo} and m_{zo} of the controlled dipole momentum for maximum angular momentum dumping of the entire wheel system are in eq. (5), where D is a scaling factor to make a unit vector.

$$\begin{aligned} m_{xo} &= (B_y\Delta\Omega_z - B_z\Delta\Omega_y)/D \\ m_{yo} &= (B_z\Delta\Omega_x - B_x\Delta\Omega_z)/D \\ m_{zo} &= (B_x\Delta\Omega_y - B_y\Delta\Omega_x)/D \end{aligned} \tag{5}$$

Considering the unmatched dipole capacities of x, y and z axes, the following rules should be applied to

the n=256 level magnetorquer controller input L. The signs of the input values are determined from the signs of dipole momentum vectors.

1. $max(|12m_{xo}|,|10.4m_{yo}|,|12m_{zo}|)$.
2. If max for x, $L_x = n$ and $L_{y,z} = nm_{y,zo} / m_{xo}$.
3. If max for y, $L_y = n$ and $L_{x,z} = nm_{x,zo} / m_{yo}$.
4. If max for z, $L_z = n$ and $L_{x,y} = nm_{x,yo} / m_{zo}$.

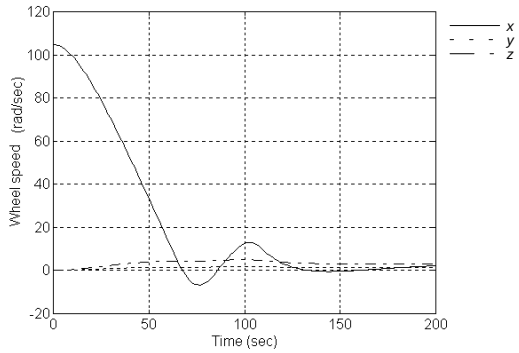

Fig. 6. Momentum dump history

Fig. 6. demonstrates the momentum dumping capability of the KITSAT-3 according to above rules. A dead band switch is employed to avoid unnecessary control efforts within an acceptable error range. Two seconds of sampling time is used from the varying geomagnetic field model and a simple PD control algorithm applied as the spacecraft control law during the dumping action.

6. ATTITUDE MANEUVERS

6.1 Control Algorithm

When the imaging mode is demanded, fast rotational maneuvers are required from the sun pointing to the Earth pointing attitude. Since large angle maneuvers are required for the three axes in a short period, the nonlinearity due to the rotational dynamics becomes dominant for the system response, so the effect cannot be avoided.

Quaternion feedback control scheme has been proposed for the three-axis large angle maneuvers, where global stability is guaranteed (Wie, 1985, 1989). Quaternions as a measure of attitude error give a simple feedback signals of the three axes. Moreover they are well suited for onboard real-time computation, since only products and no trigonometric relations exist in their kinematics equations. Four elements of quarternions are defined in eq. (6).

$$\begin{aligned} q_1 &= C_1 \sin(\phi/2) \\ q_2 &= C_2 \sin(\phi/2) \\ q_3 &= C_3 \sin(\phi/2) \\ q_4 &= \cos(\phi/2) \end{aligned} \tag{6}$$

where ϕ is the Euler axis rotation angle and $C_{1,2,3}$ are the direction cosines of the Euler axis with respect to the inertial reference frame.

The error quaternions can be expressed in terms of desired and measured quaternion values as in eq. (7).

$$\begin{bmatrix} q_{e1} \\ q_{e2} \\ q_{e3} \\ q_{e4} \end{bmatrix} = \begin{bmatrix} q_{d4} & q_{d3} & -q_{d2} & -q_{d1} \\ -q_{d3} & q_{d4} & q_{d1} & -q_{d2} \\ q_{d2} & -q_{d1} & q_{d4} & -q_{d3} \\ q_{d1} & q_{d2} & q_{d3} & q_{d4} \end{bmatrix} \begin{bmatrix} q_{m1} \\ q_{m2} \\ q_{m3} \\ q_{m4} \end{bmatrix} \tag{7}$$

where, q_{ei} = error quaternion

q_{di} = desired quaternion

q_{mi} = measured quaternion

The control laws in eq. (8) are related with the wheel momentum change in eq. (3).

$$\begin{aligned} T_{cx} &= -[K_{qe1}\, q_1 + K_{w1}\, \omega_x] = -I_w \Omega'_x \\ T_{cy} &= -[K_{qe2}\, q_2 + K_{w2}\, \omega_y] = -I_w \Omega'_y \\ T_{cz} &= -[K_{qe3}\, q_3 + K_{w3}\, \omega_z] = -I_w \Omega'_z \end{aligned} \tag{8}$$

According the above control laws 120° and 22.5° large angle maneuvers are performed in simultaneous manner about the y and x axes, respectively. Now there are six unknown gains to be selected to meet the control system requirement. Approximation of the rotational dynamics by neglecting the gyroscopic effect in eq. (3) gives the gains associated with the settling time and overshoot for the well-known linear second-order system (Wie, 1989). But these gains are not optimal for certain performance measures and the system constraints are not taken into account. The system could be unrealizable if the control parameters are over-estimated. Since the closed-loop system shows complex and nonlinear characteristic, it is hard to apply the conventional gain tuning algorithm which requires the knowledge of the system behaviors.

Recently genetic algorithm has been proposed as a searching algorithm. A genetic algorithm is useful to find out the best fitting gain vectors which satisfy the constraints if the system dynamics is complex. It provides powerful tools for solving complicated optimization problems (Goldberg, 1989). In this paper, a genetic algorithm was used for tuning the quaternions and rate gain vectors which minimize a given performance measure. The performance measure (PM) can be any function associated with the system variables. Since the system behavior cannot be described by a closed-form, the evaluation of the

performance measure is numerically evaluated.

Since the maximum generated torque and momentum storage capacity are constrained in the wheel specifications, the control algorithm has to consider the limitation. A penalty function approach is effective for solving such a constrained problem. By using a penalty function, the constrained problem can be made into a unconstrained one. Chromosomes that break the constraints are penalized by reducing their performance measures. Therefore they have little chance to be selected at the next generation.

In this paper, the performance measure (PM) is defined as the mean squares of error quaternions and penalty function.

$$PM = \sum_{i=1}^{N} \sqrt{{q_{e1i}}^2 + {q_{e2i}}^2 + {q_{e3i}}^2 + (1 - q_{e4i})^2} + \varepsilon \cdot \delta \sum_{i=1}^{P} \Phi_i \qquad (9)$$

where, N is the number of iteration

ε is -1 for maximization

+1 for minimization

δ is a penalty coefficient

Φ is a penalty related to the i_{th} constraint

P is the total number of constraints

Chromosome, which is an encoding of the solution, is defined as a real valued-vector consisting of six quaternions and rate gains. Initial population is generated randomly within the neighbourhood of the nominal gain vectors which is decided by approximation method. Two genetic operations are performed : crossover and mutation. A simple crossover is used and mutation is performed by changing the value of an element of chromosome with exponentially decreasing step size.

if (Location of mutation == i)

$step = ae^{\mathrm{PM}}$

$P(i) = P(i) \pm step$

where, $P(i)$ is the i_{th} element of chromosome and a is a constant.

The best fitting chromosome is selected from the evaluation procedure and reproduces itself as many times as the population size.

6.2 Simulation

All model parameters were given above and rotational maneuver from the Sun point to the Earth pointing attitude are assumed. Desired quaternions are the same as the Earth pointing attitude which vary according to the spacecraft movement. Initial quaternions are calculated from the Sun pointing attitude at the beginning of the eclipse.

Initial quaternions = (0.080, 0.555, 0.707, 0.430)

The nominal gain vector is calculated from the following formula (Wie, 1989):

- Settling time 60 sec = $8/(\delta\omega_n)$
- Critical damped case : $\delta = 1$
- $k/2 = \omega_n^2$
- $d = 2\delta\omega_n$
- $Kq = k I$
- $Kw = d I$

Therefore, $K_{q1} = 0.111$, $K_{q2} = 0.1086$, $K_{q3} = 0.1444$, $K_{w1} = 0.8058$, $K_{w2} = 0.8144$, $K_{w3} = 1.0827$.

Parameters for the genetic algorithm are given below :

- No. of population = 100
- Probability of crossover = 1.0
- Probability of mutation = 0.8

Fig. 7. shows the performance of error the quaternions for the nominal quaternion feedback method with 60sec settling time. As shown in Fig. 8. the x wheel exceeds the range of the nominal operation speed. To prevent this drawback, longer settling time has to be selected, which affects the fast convergence characteristic of error quaternions.

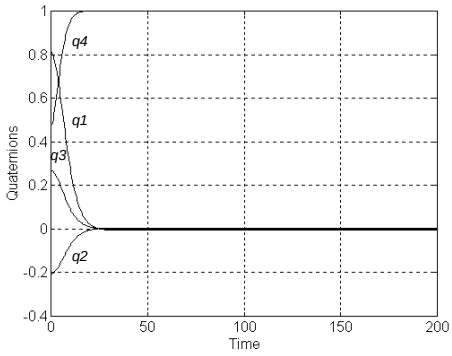

Fig. 7. Error quaternion history of nominal control case with 60 sec settling time

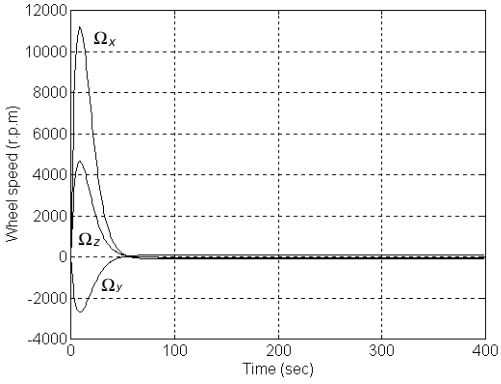

Fig. 8. Reaction wheel speeds of nominal control

The genetic method has a good convergence characteristic of error quaternions without causing overloads to the wheels. Fig. 10. and 11. are reaction wheel speeds and the generated control torques when the genetic algorithm is applied. It clearly demonstrates that the wheel speed limitation and torque capability are within the range of the specification of the reaction wheel. However, due to the time varying desired quaternions as the satellite moves around the orbit, small steady state errors exist in the error quaternions.

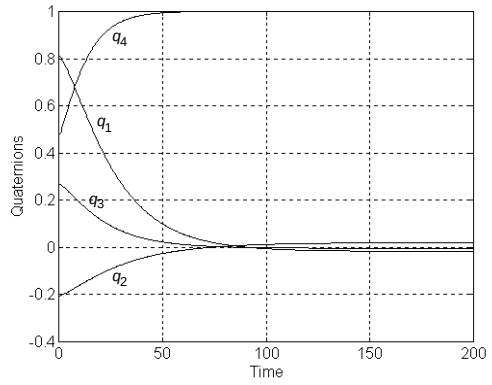

Fig. 9. Error quaternion history of genetic algorithm case

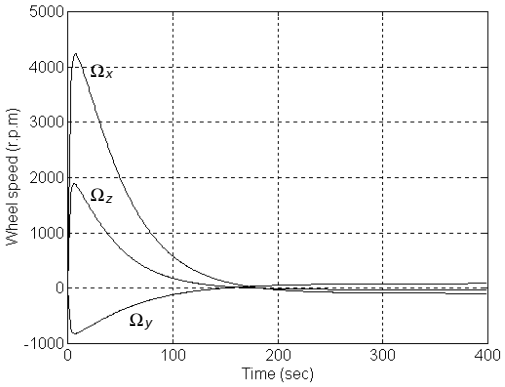

Fig. 10. Reaction wheel speeds for genetic method

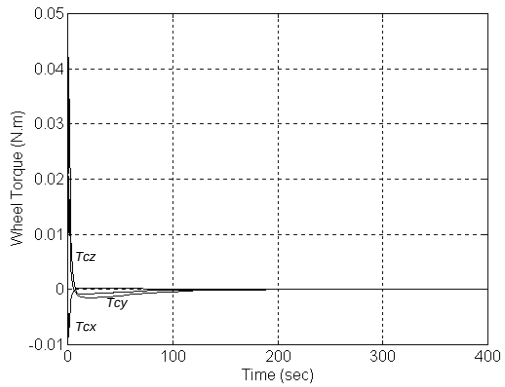

Fig. 11. Reaction wheel torques

7. CONCLUSION

As a low cost satellite the KITSAT-3 has been proposed as a highly maneuverable space platform. Environmental disturbance model and spacecraft attitude dynamics are analyzed. Momentum dumping capability by means of magnetorquering has been demonstrated with an efficient control law.

Since the spacecraft is designed under small volume and mass constraints, specially designed attitude control hardwares are selected. The genetic algorithm for searching the gain parameters developed in this paper showed satisfactory results with the given limited hardware capacities.

However, considering the desired attitude changes during the large angle maneuvering, steady state errors exist when tracking mode is demanded. To cope with the problem small angle approximation dynamics and control laws should be adopted separately. Having two different control laws according to the error can simplify the controller design and reduce the computation load of the satellite onboard microprocessor.

REFERENCES

Goldberg, D.E., (1989). *Genetic Algorithms in Search, Optimization, and Machine Learning*. Addison-Wesley Pub., Reading.

Hughes, P.C. (1986). *Spacecraft Attitude Dynamics*. John Wiley & Sons, New York.

Kaplan, M.H. (1976). *Modern Spacecraft Dynamics and Control*. John Wiley & Sons, New York.

Wie, B. and P.M. Barba (1985). *Quaternion Feedback for Spacecraft Large Angle Maneuvers*, Journal of Guidance, **8**, 360-365.

Wie, B., H. Weiss and A. Arapostathis (1989). *Quaternion Feedback Regulator for Spacecraft Eigenaxis Rotations*, Journal of Guidance, **12**, 375-380.